4ème Conférence Internationale des Energies Renouvelables CIER-2016
Proceedings of Engineering and Technology – PET
Pol.18, pp101 - 105

Associed Matrix Converter - DFIG Employed In Wind Energy Coversion System

K. Bedoud[(1)], T. Bahi[(2)], H. Merabet[(1)]
[1]*Research Center in Industrial Technologies CRTI, ex CSC, BP 64 Cheraga, Algeria.*
[2] *Automatic Laboratory and Signals, Badji Mokhtar University, Annaba, Algeria*
**BEDOUD Khouloud: khouloud1981@yahoo.fr*

***Abstract*— In this paper, we present the performance study of a variable-speed wind turbine based on doubly fed induction generator with using the maximum power point tracking methode for to extract the maximum power avaible. The control scheme is tested and the performances ares evaluated by simulation results.The simulation results obtaned under MatLab/Simulink shows the effectiveness and validity of the considered control.**

***Keywords*—Wind turbine, Control, Matrix converter, Doubly Fed Induction Generator**

I. INTRODUCTION

Wind Generation Systems (WGS) are currently taking a great interest in renewable energy systems [1] A wind turbine is a mechanical device that converts kinetic energy into mechanical energy which then is converted to electrical energy by coupling a generator to the wind turbine [02]. Currently wind energy can be used under various schemes, that is, primary source with storage systems provide energy in remote locations, as primary energy source with conventional sources to inject energy into a grid; The wind turbine can be operated at the maximum power operating point (MPPT) for various wind speeds by adjusting the shaft speed optimally to achieve maximum efficiency at all wind velocities [2-4]. Pitch angle regulation is required in conditions above therated wind speed when the rotational speed is not kept constant. Small changes in pitch angle can have a dramatic effect on the power output [5]. Wind power has become increasingly popular because of the increasing difficulty of the environmental pollution and the greenhouse effect. Huge efforts have been made in promoting the WECS, to reduce costs, increase reliability and robustness [06].Actually, in the field of renewable energies, several types of electric machines are used as generators in wind energy conversion systems (WECS) [6-8] ; Therefore, the study of double fed induction generator (DFIG) has regaind importance because he have become the most popular generators for wind energy applications.

II. WECS MODEL

The wind energy concersion system considered in this work includes the wind turbine , gearbox, double fed induction generator (DFIG), matrix converter and the electrical network. Figure 1 shows the equivalent diagram of wind energy conversion systems.

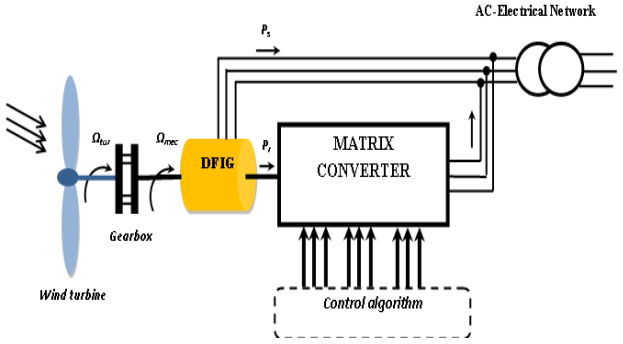

Figure1. Equivalent diagram of WECS

2.1 Modeling of wind turbine

Wind energy comes from the kinetic energy of the wind. Thus, if we consider that the mass of air (m) which moves with the velocity (V), the kinetic energy of this mass and the turbine power are given by the following relation [9]:

$$E_c = 0.5\, m\, V^2 \tag{1}$$

$$P_v = \frac{1}{2}\cdot\rho\cdot s\cdot V^3 \tag{2}$$

Where, ρ is the air density (ρ =1,25 kg/m^3), m is mass of air, V is the wind speed

Taking into account of The power coefficient (Cp) which presents the aerodynamic efficiency of the turbine and depends on the specific speed λ and the angle of the blades β. It is different from a turbine to another, and is usually provided by the manufacturer and can be used to define a mathematical approximation. The power coefficient and the specific speed are defined by [10] .

$$C_p = \left(0.45 - \left(0.0167(\beta - 2)\right)\right)\left(\sin\left(\frac{\pi(\lambda+0.1)}{(15.5-(0.3(\beta-2)))}\right)\right) - \left(0.00184(\lambda - 3)(\beta - 2)\right) \tag{3}$$

$$\lambda = \frac{R\,\Omega_{tur}}{V} \tag{4}$$

ISSN 2356-5608

4ème Conférence Internationale des Energies Renouvelables CIER-2016
Proceedings of Engineering and Technology – PET
Pol.18, pp101 - 105

So, the turbine power and torque developped are expressed respectively by [9, 10]:

$$P_w = \frac{1}{2} C_p(\lambda, \theta).\rho.\pi.R^3.V_w^3 \quad (5)$$

$$C_{tur} = \frac{P_{tur}}{\Omega_{tur}} = C_p.\frac{\rho.S.V^3}{2}.\frac{1}{\Omega_{tur}} \quad (6)$$

Figure 2 shows the computed relation between the power coefficient Cp (λ, θ) and the specific velocity, λ for different angles θ using wind turbine parameters given in appendices. It is clear from this figure λ that there is a value which ensures maximum power captured from the wind for each stall angle. For each wind speed, the machine rotates so that it captures the maximum available power. Based on previous relationships, the Power-Velocity characteristic can be plotted for different wind speeds (see Figure 3).

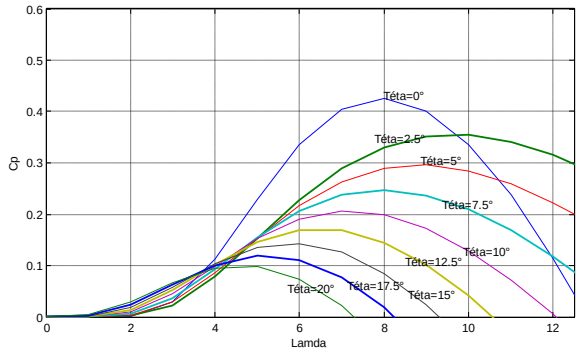

Fig. 2 Caractéristics Cp (λ, θ)

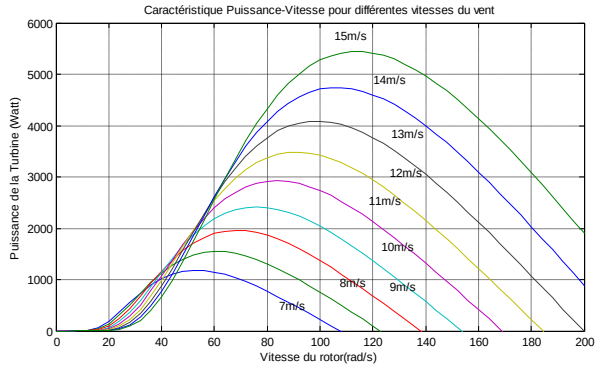

Fig. 3 Caractéristics Power-speed

The rotation speed which provide an extraction of the maximum powers are calculated as a function of the optimum specific velocity λ and the stall angle θ. These speeds are given in the table Tab. 1

Wind speed (m/s)	P (°)								
	0	2.5	5	7.5	10	12.5	15	17.5	20
0	0	0	0	0	0	0	0	0	0
2	19.2	24	21.6	19.2	16.8	14.4	14.4	12	9.6
4	**38.4**	**48**	**43.2**	**38.4**	**33.6**	**28.8**	**28.8**	**24**	**19.2**
6	57.6	72	64.8	57.6	50.4	43.3	43.3	36	28.8
8	76.8	96	86.4	76.8	67.2	57.6	57.6	48	38.4
10	96	120	108	96	84	72	72	60	48
12	115.2	144	129.6	115.2	100.8	86.4	86.4	72	57.6
14	134.4	168	151.2	134.4	117.6	100.8	100.8	84	67.2
16	144	180	162	144	126	108	108	90	72
	W_m (rd/s)								

Tab. 1. Rotation speed

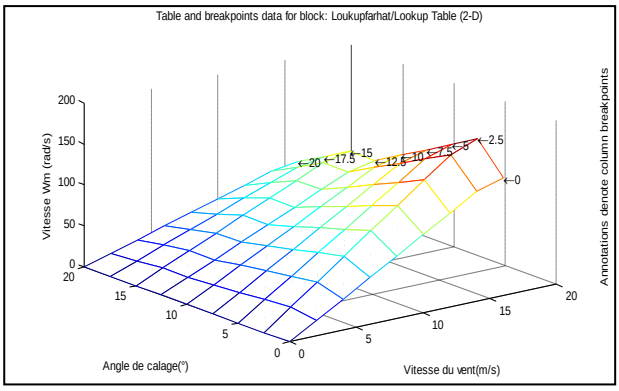

Fig. 4 Data table 2-D for the speed DFIG

The mechanical part of the wind turbine can be presented as follows:

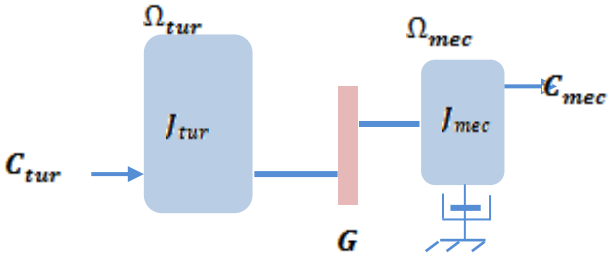

Fig. 5 Mechanical part of wind turbine

The wind turbine shaft is connected to the WFSG rotor through a gearbox which adapts the slow speed of the turbine to the WFSG speed. This gearbox is modeled by the following equations [11]:

$$\Omega_{mec} = G.\Omega_{tur} \quad (7)$$

Where,

$$G = \frac{C_{tur}}{C_{mec}} \quad (8)$$

From the dynamics fundamental relation, the turbine speed is determined as follows:

$$J\frac{d\Omega_{mec}}{dt} = C_{mec} - C_{em} - f\Omega_{mec} \quad (9)$$

J and f are the total moment of inertia and the viscous friction coefficient appearing at the generator side, C_{mec} is the gearbox torque, Cem is the generator torque, and Ω_m is the mechanical generator speed.

Figure 6 shows the block diagram of the wind turbine shaft

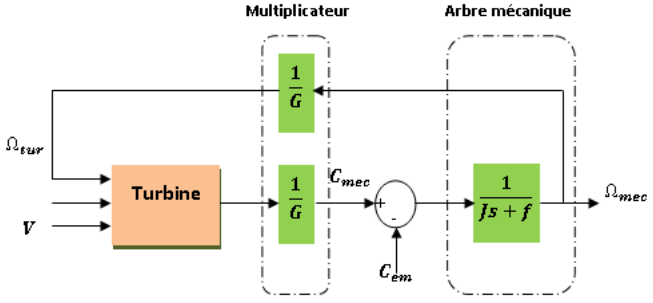

Fig. 6 Wind Turbine Model

4ème Conférence Internationale des Energies Renouvelables CIER-2016
Proceedings of Engineering and Technology – PET
Pol.18, pp101 - 105

2.2 Doubly fed induction generator model

2.2 Doubly fed induction generator model

The mathematical model of DFIG can be given by the following equations [12-14] :

$$\begin{cases} V_{ds} = R_s i_{ds} + \dfrac{d\phi_{ds}}{dt} - w_s \phi_{qs} \\ V_{qs} = R_s i_{qs} + \dfrac{d\phi_{qs}}{dt} + w_s \phi_{ds} \\ V_{dr} = R_r i_{dr} + \dfrac{d\phi_{dr}}{dt} - (w_s - w_r).\phi_{qr} \\ V_{qr} = R_r i_{qr} + \dfrac{d\phi_{qr}}{dt} + (w_s - w_r).\phi_{dr} \end{cases} \quad (10)$$

$$\begin{cases} \phi_{ds} = L_s i_{ds} + M i_{dr} \\ \phi_{qs} = L_s i_{qs} + M i_{qr} \\ \phi_{dr} = L_r i_{dr} + M i_{ids} \\ \phi_{qr} = L_r i_{qr} + M i_{qs} \end{cases} \quad (11)$$

$$C_e = 3p\frac{M}{2}(i_{dr} i_{qs} - i_{qr} i_{ds}) \quad (12)$$

where V_{sd} ,V_{sq} ,V_{rd} and V_{rq} are the stator and rotor d-q axes voltages, respectively; Rs and Rr are the stator and rotor phase resistances, respectively; I_{sd} ,I_{sq} ,I_{rd} and I_{rq} are the stator and rotor d-q axes currents, respectively; $\psi_{sd} - \psi_{sq}$ and $\psi rd - \psi rq$ are the stator and rotor d-q axes fluxes, respectively; L_s, L_m, and Lr are the stator, magnetizing, and rotor inductances, respectively; ω_e and ω_r are the synchronous and rotating angular frequencies, respectively; Te is electromagnetic torque; and P is number of poles.

2.3 Matrix converter model

The MC structure is shown in Figure 7. It is formed of bidirectional elements.

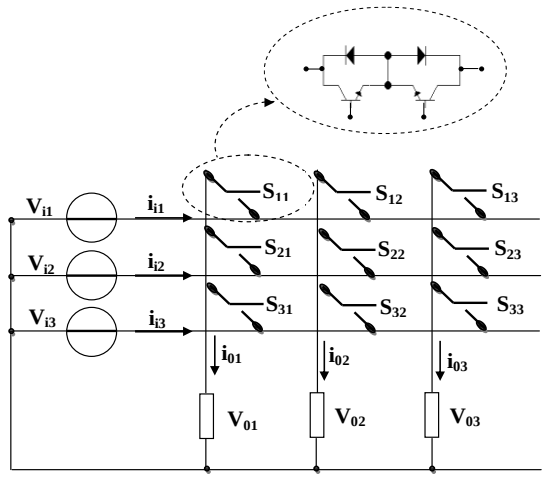

Fig.7 MC converter structure

The input and output voltages are expressed in the following matrix forms:

$$[V_o(t)] = [M(t)].[V_i(t)] \text{ and } [I_i(t)] = [M(t)].[I_o(t)] \quad (13)$$

With,

$$[M(t)] = \frac{1}{3}.\begin{bmatrix} 1+2.q.\cos(w_m t) & 1+2.q.\cos\left(w_m t - \frac{2\pi}{3}\right) & 1+2.q.\cos\left(w_m t - \frac{4\pi}{3}\right) \\ 1+2.q.\cos\left(w_m t - \frac{4\pi}{3}\right) & 1+2.q.\cos(w_m t) & 1+2.q.\cos\left(w_m t - \frac{2\pi}{3}\right) \\ 1+2.q.\cos\left(w_m t - \frac{2\pi}{3}\right) & 1+2.q.\cos\left(w_m t - \frac{4\pi}{3}\right) & 1+2.q.\cos(w_m t) \end{bmatrix} \quad (14)$$

With,

$$w_m = w_o - w_i \quad (15)$$

Where,

q : transformation ratio between the input and output voltage.

I_{im} : input current ;

I_{om} : output current ;

φ_i : Phase between the voltage and the current at the input ;

φ_o : Phase between the voltage and the current at the output

The three phases consist of 3x3 switches. Which have 512 combinations of switching states with only 27 states are possible[15]. Considering:

- To avoid short circuit: do not connect two input lines to the same (most common) output line;
- To avoid an open circuit of loads: do not disconnect the output line (surge circuits)

The elements of the connection matrix [M (t)], are defined as follows:

$$m_{kj} = \frac{t_{kj}}{T_{sdq}} = \frac{1}{3}.\left[1 + 2.\frac{V_{ik}.V_{oj}}{V_{im}^2}\right] \quad (16)$$

Avec k=1, 2,3 et j=1, 2,3.

4ème Conférence Internationale des Energies Renouvelables CIER-2016
Proceedings of Engineering and Technology – PET
Pol.18, pp101 - 105

$$m_{kj} = \frac{t_{kj}}{T_{séq}} = \frac{1}{3}.\left[1 + 2.\frac{V_{ik}.V_{oj}}{V_{im}^2} + \frac{4.q}{3\sqrt{3}}sin(w_i t - \beta_k).sin(3w_i t)\right] \quad (17)$$

Avec k=1, 2,3 ; j=1, 2,3 et $\beta_k = 0, \frac{2\pi}{3}, \frac{4\pi}{3}$.
The sequence time is:

$$T_{séq} = t_{11} + t_{21} + t_{31} = t_{12} + t_{22} + t_{32} = t_{13} + t_{23} + t_{33} \quad (18)$$

Where, $t_{11}, t_{21}, \ldots\ldots\ldots t_{33}$ are defined, respectively , as the conduction time of $S_{11}, S_{21}, \ldots\ldots\ldots S_{33}$ During a sequence.

The switching time of the switch which connects the input phase k to the output phase j is then defined by the following equation:

$$t_{kj} = T_{séq}.\left[\frac{1}{3} + 2.\frac{V_{ik}V_{jréf}}{3.V_{im}^2} + \frac{4.q}{9\sqrt{3}}sin(w_i t - \beta_k).sin(3w_i t)\right] \quad (19)$$

Where, $V_{jréf}$ is the desired output voltage.

$$V_{jréf} = q.V_{im}.cos(w_o t - \beta_j) - \frac{q}{6}.V_{im}cos(3w_o t) + \frac{q}{4q_m}.V_{im}cos(3w_i t). \quad (20)$$

Avec $\beta_j = 0, \frac{2\pi}{3}, \frac{4\pi}{3}$

Therefore, the state of the switches can be written as follows:

$$\begin{cases} S_{11} = 1\ si\ n.T_{séq} \ll t \ll t_{11} + n.T_{séq} \\ S_{21} = 1\ si\ n.T_{séq} + t_{11} \ll t \ll t_{11} + t_{21} + n.T_{séq} \\ S_{31} = 1\ si\ n.T_{séq} + t_{11} + t_{21} \ll t \ll t_{11} + t_{21} + t_{31} + n.T_{séq} \end{cases} \quad (21)$$

$$\begin{cases} S_{12} = 1\ si\ n.T_{séq} \ll t \ll t_{12} + n.T_{séq} \\ S_{22} = 1\ si\ n.T_{séq} + t_{12} \ll t \ll t_{12} + t_{22} + n.T_{séq} \\ S_{32} = 1\ si\ n.T_{séq} + t_{12} + t_{22} \ll t \ll t_{12} + t_{22} + t_{32} + n.T_{séq} \end{cases} \quad (22)$$

$$\begin{cases} S_{13} = 1\ si\ n.T_{séq} \ll t \ll t_{13} + n.T_{séq} \\ S_{23} = 1\ si\ n.T_{séq} + t_{13} \ll t \ll t_{13} + t_{23} + n.T_{séq} \\ S_{33} = 1\ si\ n.T_{séq} + t_{13} + t_{23} \ll t \ll t_{13} + t_{23} + t_{33} + n.T_{séq} \end{cases} \quad (23)$$

$n = 1,2,3, \ldots\ldots\ldots\ldots$ is the sequence number

To validate the algorithm, the figures 8a and 8b shows and phase voltage of output for frequencies (25Hz and 75Hz).

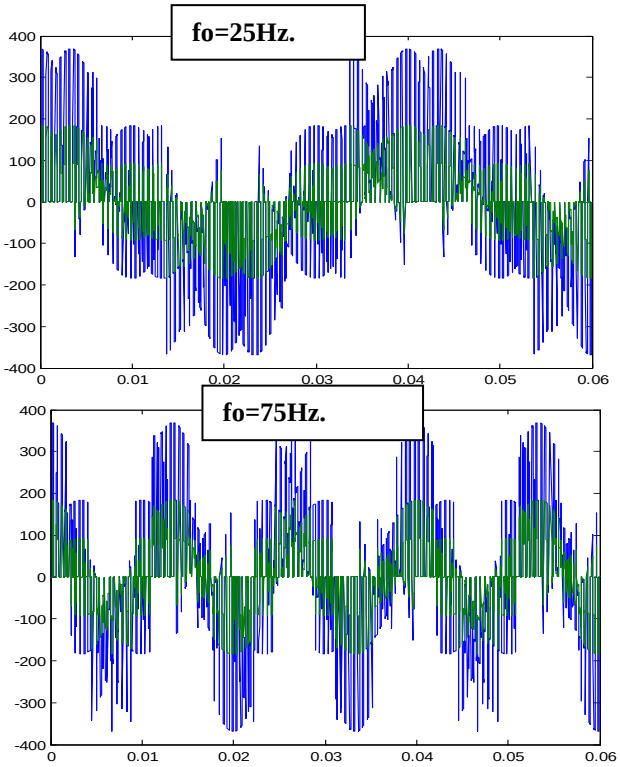

Fig.8. Simple output voltage (Green) et phase output voltage (Blue)

III. STRUCTURE OF THE CONTROL

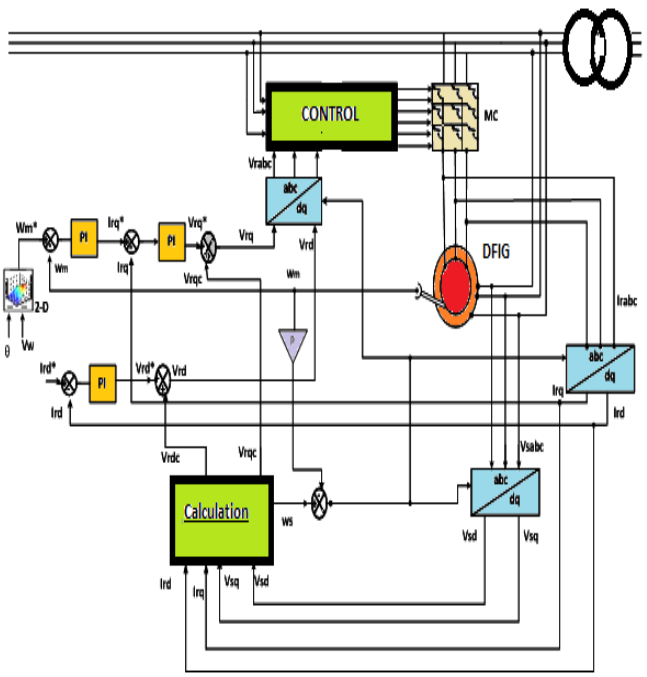

4ème Conférence Internationale des Energies Renouvelables CIER-2016
Proceedings of Engineering and Technology – PET
Pol.18, pp101 - 105

4. Simulation results

The studied system , shows in Figure 9, is simulated using MatLab/Simulink. After presenting the structures and modules of the different parts of the chain, we developed a program under the Matlab Simulink software and analyze the functioning of the system. The simulation was performed with the Matlab / Simulink software to validate the commands studied in this work.The wind profile used in simulations is constant 8m/s and the reference reactive power is variable. The decoupling effect of the between the active and reactice power of the wind energy conversion systems is illustrated in Figure 10 and Figure 11 for rotor and stator. Each parameter perfectly follows its reference value with a very good in dealing with the time-varying,

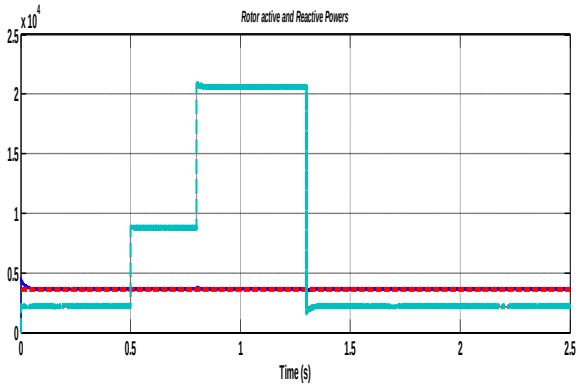

Fig. 10 Rotor active and rective powers

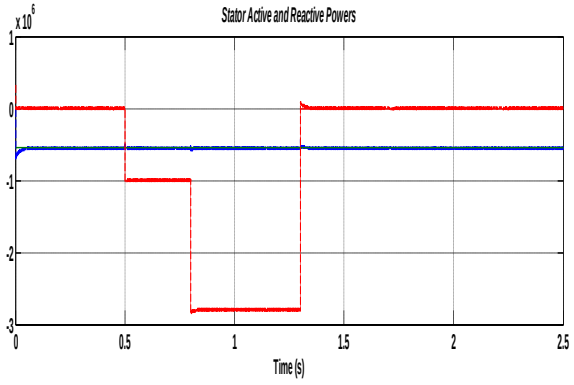

Fig. 11 Stator active and rective powers

5. Conclusion

In this paper, the modelling and control of a wind system with variable speed wind turbine are considered. The control is applied apply independent control of active power and reactive generated by the wind energy conversion system based on on doubly fed induction generator are controlled. The model of the wind conversion chain is developed and the technique of maximum power point tracking is applicate to provide all of the active power generated to the grid with unity power factor. The results showed that the active and reactive power of the wind energy.

References

[1] O. Carranza, E. Figueres, G. Garcerá, R. Ortega, C.L. Trujillo, « Study of the control structure of a small wind turbine with permanent magnet synchronous generator", IEEE 2012.

[2] T.Senjyu, R. Sakamoto, N. Urasaki, T. Funabashi, and H. Sekine, « Outpout Power Leveling of Wind Farm Using Pitch Angle Control with Fuzzy Neural Network », IEEE Power Electron. Conf., 2006.

[3] G.Ramtharan, J.B. Ekanayake and N. Jenkins, Frequency Support from Doubly Fed Induction Generator Wind Turbines , IET Renew. Power. Gener., vol. 1, no.1, pp. 3-9, 2007.

[4] S. Morimoto, H. Nakayama, M. Sanada, and Y. Takeda, « Sensorless Output Maximization Control for Variable-Speed Wind generation System Using IPMSG », IEEE Trans. Ind. Appl., vol 41, no. 1, pp. 60-67, Jan/Feb 2005.

[5] J. Zhang, M. Cheng, Z. Chen, and X. Fu, « Pitch Angle Control for Variable Speed Wind Turbines », DRPT2008 6-9 April 2008 Nanjing China .

[6] M. Cheng, Y. Zhu, « The state of the art of wind energy conversionsystems and technologies: A review», Energy Convers. Manage. , vol. 88, pp. 332-347, Dec. 2014.

[7] Tahir Khalfallah, Belfadal Cheikh, Allaoui Tayeb, Gerard Champenois, « Power control of wind turbine based on fuzzy sliding mode control», International journal of power electronics and drive system (IJPEDS), V.5, N°4, April 2015, pp : 502-511

[8] Blaabjerg F, Iov F, Chen Z, Ma K. , « Power electronics and controls for wind turbine systems»,IEEE International Energy Conference and Exhibition. pp : 333-344, 2010.

[9] Y.Mastanamma, S.Deepthi, « Harmonic Analysis of Conversion Systems Using MATLAB/Simulink», International Journal of Advanced Research in Electrical,Electronics and Instrumentation Engineering, Vol. 4, Issue 5, May 2015.

[10] Khouloud Bedoud , Mahieddine Ali-rachedi , Tahar Bahi , Rabah Lakel b, Azzeddine Grid, « Robust Control of Doubly Fed Induction Generator for Wind Turbine Under Sub-Synchronous Operation Mode»,Energy Procedia 74 (2015) 886 – 899, ScienceDirect 1876-6102 © 2015 Published by Elsevier Ltd.

[11] Belabbas B, Tayeb A, Mohamed T, Ahmed S, « Hybrid Fuzzy Sliding Mode Control of a DFIG Integrated into the Network», International Journal of Power Electronics and Drive System (IJPEDS). 2013; 3(4); 351-364.

[12] H. Altun et S. Sunter « Modeling, simulation and control of wind turbine driven doubly-fed induction generator with matrix

converter on the rotor side». Electr Eng(2013) pp 157-170 springer-verlag 2012

[13] Jiawei Chen, JieChen , and Chunying Gong, « New Overall Power Control Strategy for Variable-Speed Fixed-Pitch Wind Turbines Within the Whole Wind Velocity Range ». IEEE Transactions on Industrial Electronics, vol. 60, no. 7, july2013.

[14] Huseyin Altun, Sedat Sunter, « Modeling , similation and control of wind turbine driven doubly-fed induction generator with matrix converter on the rotor side », Electr Eng ,n° 95 ,pp , 157 :170, 2013.

[15] P.Wheeler, J.Rodriguez, J.C Clare, L. Empringham and A. Weintein,« Matrix converters a technology review », IEEE Transaction on Industrial Electronics, Vol 49, pp276-288, 2002.